Korean J. Chem. Eng., 34(6), 1813-1821 (2017)
DOI: 10.1007/s11814-017-0049-6

pISSN: 0256-1115
eISSN: 1975-7220

Developing thin film heterogeneous ion exchange membrane modified by 2-acrylamido-2-methylpropanesulfonic acid hydrogel-co-super activated carbon nanoparticles coating layer

Mahsa Nemati*, Sayed Mohsen Hosseini*,†, and Meisam Shabanian**

*Department of Chemical Engineering, Faculty of Engineering, Arak University, Arak 38156-8-8349, Iran
**Faculty of Chemistry and Petrochemical Engineering, Standard Research Institute, Karaj 31745-139, Iran
(*Received 12 August 2016 • accepted 27 February 2017*)

Abstract−Highly selective cation exchange membranes were prepared by coating a thin 2-acrylamido-2-methylpropanesulfonic acid based hydrogel layer and super activated carbon nanoparticles-co-hydrogel layer on polyvinyl chloride based cation exchange membranes. FTIR analysis proved hydrogel formation on membrane surface successfully. Scanning electron microscopy images and swelling ratio measurement were used to study the effect of super activated carbon nanoparticles on properties of formed hydrogel. The surface morphology, surface hydrophilicity and roughness analysis were also used in membrane characterization. Membrane water content was increased by formation of modified layer on the membranes surface. Modified membranes showed a remarkable improvement in potential, permselectivity and transport number compared to pristine type. Membrane ionic flux and permeability were improved initially by using modifier layer on membrane surface, and then showed decreasing trend at high nanoparticles loading ratios in hydrogel layer. Modified membranes showed lower electrical resistance compared to unmodified membrane.

Keywords: Cation Exchange, Thin Film, Coating Layer, Hydrogel, Super Activated Carbon Nanoparticles

INTRODUCTION

One of the main challenges of concern in the modern world is water purification, due to the increasing human population and limited water resources [1-4]. Membrane water treatment is expected to be a promising method in areas such as drinking water treatment, brackish and seawater desalination, and wastewater treatment [4]. Electrodialysis (ED) is a separation technology that utilizes ion exchange membranes (IEMs) for production of potable water from brackish water under an electrical driving force [5,6]. IEMs are also utilized as active separators in other electrochemical processes where selective transport of charged particles is required, such as sodium chloride concentration for chlor-alkali industry, removal of specific cations from industrial effluent, waste water treatment, pH adjustment, heavy metal removal, reverse electrodialysis (RED) and many more processes [6-14]. However, scientists must improve the electrochemical properties of ion exchange membranes such as ion selectivity and conductivity, ionic permeability and flux, thermal, mechanical and chemical stabilities to make electrodialysis more effective and applicable [5,8,12,15,16]. Numerous methods to modify ion exchange membranes have been examined to improve the membrane performance. These methods have resulted in incorporation of highly adsorptive and/or hydrophilic nanomaterials into membrane structure, functionalizing the incorporated nanomaterials, polymers blending and using various ionic functional groups, etc. [2,15,17].

Moreover, many researches have been carried out to change the surface hydrophilicity, adsorptive capacity, roughness, antifouling and charge of membranes [1,14,17-20]. The methods include surface modification by grafting hydrophilic monomers by chemical treatment (e.g., UV or plasma treatment), self-assembled monolayer and thin-film coating [3,18-21].

Among the surface modification techniques, surface coating has been widely adopted to modify the properties of different membrane types, thereby achieving the desired separation performance and characteristics [16-18]. In fact, it can be a proportional way to introduce functional groups to membrane surface and increase the hydrophilicity and separation performance of membranes without affecting its matrix. In such a process, a coating layer is attached to the membrane surface physically without interfering with the chemistry of selective layer [19,22-25].

Super absorbent hydro-gels consist of chemically or physically cross-linked network of flexible chains that carry functional ionic groups. Upon contact with water, super absorbent ionic polymer networks absorb water up to several hundred times of their dry weight. Hydrogels based on polysaccharides, polyvinyl alcohol, cellulose acetate and carboxymethyl cellulose have been widely used as medical, tissue engineering, drug delivery systems, sanitary products etc. [2,26-29]. When immersed in an aqueous environment, the functional ionic groups change into negatively charged groups, enabling gel to interact with cationic ions so they seem to have the capacity to get in wastewater treatment applications [27,30].

Activated carbon is one of the promising materials in different fields such as porous electrodes, hydrogen storage and environmental remediation, which is related to good chemical stability, large surface area and high pore distribution, availability, excellent adsorp-

†To whom correspondence should be addressed.
E-mail: Sayedmohsen_Hosseini@yahoo.com, S-Hosseini@araku.ac.ir

tion properties and low cost [31-33]. The capacity of activated carbon in heavy metal ions and organic materials removal is markedly highlighted in different reports, which clarifies its utilization in membrane bioreactors and surface water decontamination as an effective sorption barrier [34-37].

In the current study, we prepared novel cation exchange membranes by coating a composite thin layer consist of network structure of 2-acrylamido-2-methylpropanesulfonic acid based hydrogel (AMAH) and super activated carbon nanoparticles on polyvinylchloride based substrate. Pristine cation exchange membranes based on polyvinylchloride were prepared through solution casting technique using tetrahydrofuran as the solvent and resin particles as functional groups agents. The modification step was preceded by coating a thin layer of composite hydrogel with different percentage of super activated carbon nanoparticles on the surface of prepared membranes.

MATERIALS AND METHODS

1. Materials

Polyvinylchloride (PVC, grade S-7054, density: 460 g/lit, viscosity number: 105 cm^3/g) supplied by Bandar Imam Petrochemical Company, Iran, was used as membrane matrix. Tetrahydrofuran (THF) (Mw: 72.11 g/mol, density: 0.89 g/cm^3) was employed as solvent. Super activated carbon (SAC) nanoparticles (100 nm, Bamboo as Raw Materials, purity >99.5%) (Merck Inc.), cation exchange resin (Ion exchanger Amberlyst® 15, strongly acidic cation exchanger, H^+ form more than 1.7 meq/g dry, density 0.6 g/cm^3, particle size: 0.355-1.18 mm) (Merck Inc.) were used in membrane preparation. 2-acrylamido-2-methylpropanesulfonic acid, 99% (AMPS) (Sigma-Aldrich), N, N′-Methylene-bis-acrylamide, 99% (MBA) (Sigma-Aldrich), ammonium persulfate, ≥98 (APS) (Mw: 228.20) (Sigma-Aldrich) were utilized. All other chemicals were supplied by Merck Inc, Germany. Distilled water was used throughout the experiment.

2. Preparation of Heterogeneous Cation Exchange Membrane

Heterogeneous cation exchange membranes were prepared based on polyvinylchloride by solution casting technique. Cation exchange resin powder was used as functional group agent and tetrahydrofuran as solvent. Membrane preparations steps are listed as follows: 1) Drying the resin particles in oven (SANEE. V. S. Co.) at 30 °C for 48 h, then pulverizing into fine particles in a ball mill (Pulverisette 5, Fritisch Co.) and sieving to the desired mesh size (−300 to +400 mesh). 2) Dissolving polymers binder (PVC) into solvent (THF : PVC, (20 : 1) (v/w)) in a glass reactor equipped with a mechanical stirrer (Model: Velp Sientifica Multi 6 stirrer) for more than 4 h. 3) Dispersing grinded resin particle (Resin: PVC, 1 : 1 (w/w)) in the polymeric solution. 4) To break up particle aggregations, the mixture was mixed vigorously at room temperature for an hour, sonicated for 30 min using an ultrasonic instrument, and then the mixing process was repeated for another 10 min using a mechanical stirrer. The mixture was cast onto a clean and dry glass plate at 25 °C, and the membranes were dried at ambient temperature (~25 °C) until solvent evaporated and solidification was done totally. Then, the polymeric films were immersed in distilled water. The composition of the base membrane and sur-

Table 1. The composition of pristine cation exchange membrane and surface modification layer

Membrane	(PVC+Resin) (w/w): (AMAH+gSAC) (w/w)
Sample 1 (M_1)	(50+50)/0
Sample 2 (M_2)	(50+50)/(100+0.00)
Sample 3 (M_3)	(50+50)/(100+0.02)
Sample 4 (M_4)	(50+50)/(100+0.05)
Sample 5 (M_5)	(50+50)/(100+0.10)
Sample 6 (M_6)	(50+50)/(100+0.30)
Sample 7 (M_7)	(50+50)/(100+0.50)

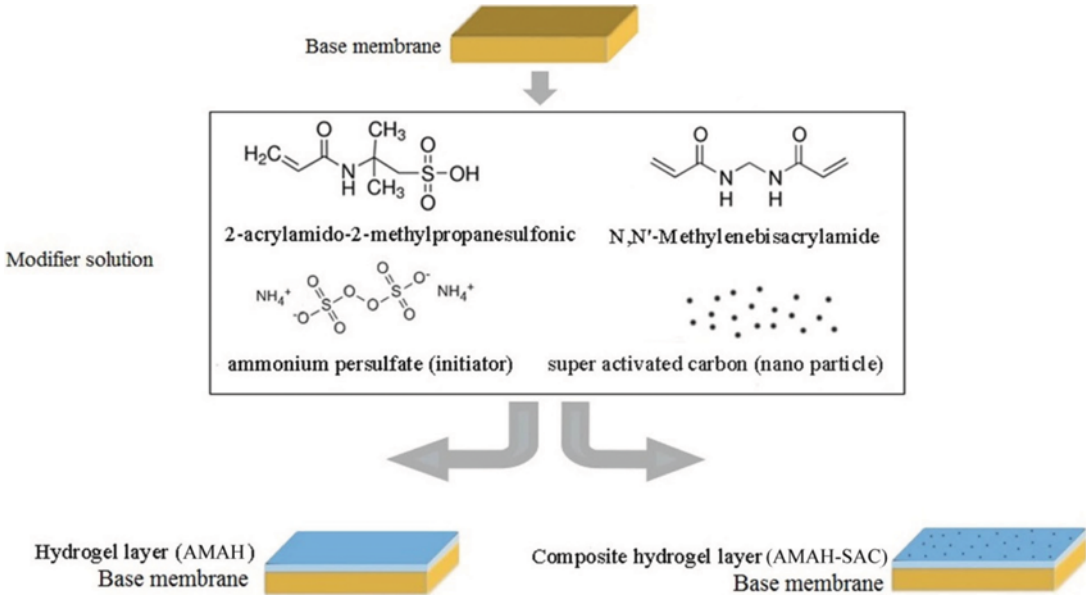

Fig. 1. The schematic diagram of coating procedure on membrane surface.

face modifier layer is given in Table 1.

3. Surface Modification by Coating with Thin 2-Acrylamido-2-methylpropanesulfonic Acid Based Hydrogel (AMAH) Layer

3 g AMPS was dissolved in 15 mL distilled water at room temperature, afterwards 0.03 g MBA (cross-linker) and 1 mL solution of APS in water (30%wt) was added to the solution. The reaction mixture was stirred at room temperature for 30 min. Then SAC nanoparticles (0.00, 0.02, 0.05, 0.10, 0.30, 0.50%wt) (SAC to AMPS) were added to the solution. The prepared mixture was poured on the upper surface of base heterogeneous membranes and rolled by a soft roller to eliminate any bubble and make a uniform area. After that, membranes were placed between two glass plates and sealed with polypropylene tape to prevent any loss of the monomers. Then the membranes were heated at 80 °C for 20 min in an oven (SANEE V. S. Co.) and washed thoroughly with distilled water. Finally, the membrane was washed sufficiently. The coating procedure with 2-acrylamido-2-methylpropanesulfonic acid based hydrogel (AMAH) layer is shown schematically in Fig. 1.

4. Test Cell

A laboratory test cell was used to measure the electrochemical properties of prepared membranes, as reported earlier [16].

5. Characterization of Hydrogel Layer

5-1. FTIR Analysis

Spectra measurements were carried out to prove the formation of AMAH/SAC nanoparticles on membrane surface. FTIR spectra analysis was done using Galaxy series FTIR 5000 spectrometer. Scans were taken with 4 cm^{-1} resolutions between 400 and 4,000 cm^{-1}.

5-2. Hydrogel Morphological Analysis

To observe the internal morphology of the prepared hydrogel and composite hydrogel, scanning electron microscope (SEM, SU3500) was employed. The as-prepared hydro gels were dried in oven (SANEE. V. S. Co.) At 30 °C for 48 h to remove any adsorbed water then frozen in liquid nitrogen. Prior to analysis, the hydrogels were sliced carefully and adhered on a copper stub, followed by being coated with gold.

5-3. Hydrogel Swelling Measurements

The prepared hydrogels (AMAH and AMAH/SAC nanoparticles) were weighted (after drying in oven at 30 °C for 48 h), then immersed in distilled water at room temperature until swelling equilibrium was achieved. Finally, the swollen hydrogels were weighed. The swelling ratio was counted by the following equation [27], where W_s and W_d(g) are the weights of the swollen hydrogels and the dried gels, respectively.

$$\text{Swelling } \% = \frac{(W_s - W_d)}{W_d} \tag{1}$$

6. Membrane Characterization

6-1. Surface Morphological Study

6-1-1. Contact Angle and Surface Roughness

Surface hydrophilicity and roughness are two effective factors on membrane behavior. Water contact angle, which is the indicator of membrane surface hydrophilicity, is a surface property affected by surface roughness, porosity and composition. The surface hydrophilicity of the prepared membranes was determined by contact angle analyzer by deposition of ionized water droplet on the membrane surface [38]. The membrane surface roughness was investigated using 3D surface image metrology software.

6-1-2. Scanning Electron Microscope (SEM)

The modified membranes containing thin coated layer were examined by scanning electron microscope (SEM, SU3500) to confirm the film formation on the membrane surface. For the membranes scanning by SEM device, the samples were frozen in liquid nitrogen and then were cut to keep the original structure. The surface SEM images of the unmodified and modified membranes were also examined. The prepared samples were coated with a thin layer of gold after mounting on a double- sided carbon tape. After sputtering with gold, their observation was undertaken by using the electron microscope.

6-2. Water Content

The membrane water content is the weight difference between the dried and swollen membranes. The membranes were immersed in distilled water for 48 h, then weighed (OHAUS, PioneerTM, Readability: 10^4 g, OHAUS Corp.) to get the dry membrane, then they were dried in oven at 60 °C until the constant weight was obtained. Following equation [38-41] can be used to calculate membrane water content:

$$\text{Water content}\% = \left(\frac{W_{wet} - W_{dry}}{W_{dry}}\right) \times 100 \tag{2}$$

To minimize the experimental errors, measurements were repeated three times and then the average values were reported.

6-3. Membrane Potential, Transport Number and Permselectivity

The membrane potential is defined as the algebraic sum of Donnan and diffusion potentials. It is determined by the partition of ions into the pores as well as the mobility of ions within the membrane phase compared with the external phase [41-46]. This parameter was evaluated for the equilibrated membrane at room temperature with unequal concentrations of electrolyte solution ((NaCl (0.1 M/0.01 M) on each sides of membrane. During the experiment, both sections were stirred constantly to minimize the effect of boundary layers and concentration polarization. The obtained potential across the membrane was measured by connecting both compartments to a saturated calomel electrode (through KCl bridges) and digital auto multi-meter (DEC, Model: DEC 330FC, Digital Multimeter, China). The measurement was repeated until a constant value was obtained. The membrane potential ($E_{Measure}$) is expressed by using Nernst equation [39,42-50] as follows:

$$E_{Measure} = (2t_i^m - 1)\left(\frac{RT}{nF}\right)\ln\left(\frac{a_1}{a_2}\right) \tag{3}$$

where t_i^m is transport number of counter ions in membrane phase, R is gas constant, T is the temperature, n is the electrovalence of counter-ion, a_1, a_2 are solutions electrolyte activities in contact membrane surfaces and F is faraday constant. The ionic permselectivity of membranes also is quantitatively expressed based on the migration of counter-ion through the IEMs [45-49]:

$$P_s = \frac{t_i^m - t_0}{1 - t_0} \tag{4}$$

where, t_0 is the transport number of counter ions in solution [47].

6-4. Ionic Permeability and Flux

During the experiment, cations pass through the membrane and

reach to the cathodic section. As anodic and cathodic reactions occur, a hydroxide ion is produced in the cathodic section per each transported sodium ion. So, the amount of transported sodium ions is equal to the produced hydroxide ions, which increases the pH of cathodic section.

$$2H_2O+2e^- \rightarrow H2\uparrow+2OH^- \text{ (Cathodic reaction)} \quad (R\text{-}1)$$

$$2Cl^- \rightarrow Cl_2\uparrow+2e^- \text{ (Anodic reaction)} \quad (R\text{-}2)$$

Ionic permeability and flux were measured using the electrodialysis test cell for Na ions. A 0.1 M (NaCl) solution was poured on one side of the two compartments test cell and a 0.01 M solution on another side. A DC electrical potential (Dazheng, DC power supply, Model: PS-302 D) with an optimal constant voltage was applied across the cell with stable platinum electrodes.

According to the first Fick's law, the flux of ions through the membrane can be expressed as follows [15,16,39,46]:

$$N = P\frac{C_1 - C_2}{d} \quad (5)$$

where, P is coefficient diffusion of ions, d is membrane thickness, N is ionic flux and C is the cation concentration in the compartments.

$$N = -\frac{V}{A}\times\frac{dC_1}{dt} = P\frac{C_1 - C_2}{d} \quad (6)$$

$$C_1^0=0.1M,\ C_2^0=0.01M,\ C_1+C_2=C_1^0+C_2^0=0.11M \quad (7)$$

where, A is the membrane surface area. Integrating Eq. (6) was as follows:

$$\ln\frac{(C_1^0+C_2^0-2C_2)}{(C_1^0-C_2^0)} = -\frac{2PAt}{Vd} \quad (8)$$

So, the flux of sodium ions/cations (N) is measured by using of titration method directly or by Digital pH-meter (Jenway, Model: 2710) through considering pH changes in cathodic section. Diffusion coefficient (P) is also calculated from Eq. (8) [15,39,41].

6-5. Electrical Resistance

The electrical resistance of equilibrated membrane was measured in NaCl solution with 0.5 M concentration (at 25 °C). Measurements were conducted by an alternating current bridge with 1,470 Hz frequency (Audio signal generator, Electronic AfzarAzma Co. P.J.S). The membrane resistance was calculated using the different resistance between the cell (R_1) and electrolyte solution (R_2) ($R_m=R_1-R_2$) [11,15,41]. The areal resistance was expressed as follows:

$$r=(R_mA) \quad (9)$$

where, r is areal resistance and A is the surface area of membrane.

RESULTS AND DISCUSSION

1. FT-IR Spectra Analysis

Fig. 2 shows spectra of the bare heterogeneous PVC membrane, 2-acrylamido-2-methylpropanesulfonic acid based hydrogel and PVC based heterogeneous membrane coated with 2-acrylamido-2-methylpropanesulfonic acid based hydrogel layer.

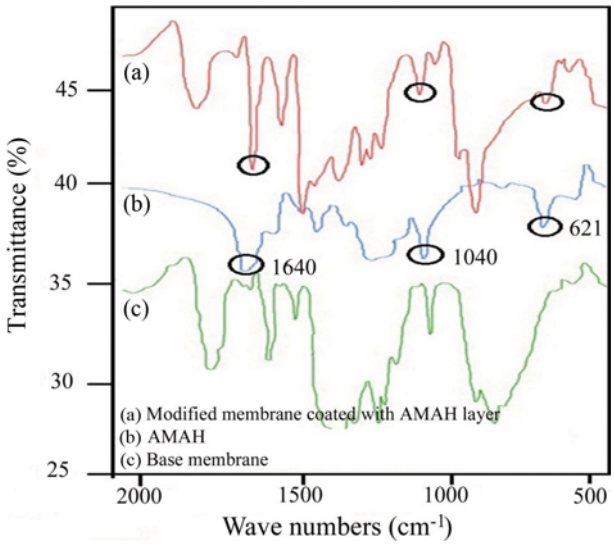

Fig. 2. The FTIR spectrum analysis of prepared membranes: PVC based membrane, AMAH and modified membrane by AMAH thin layer.

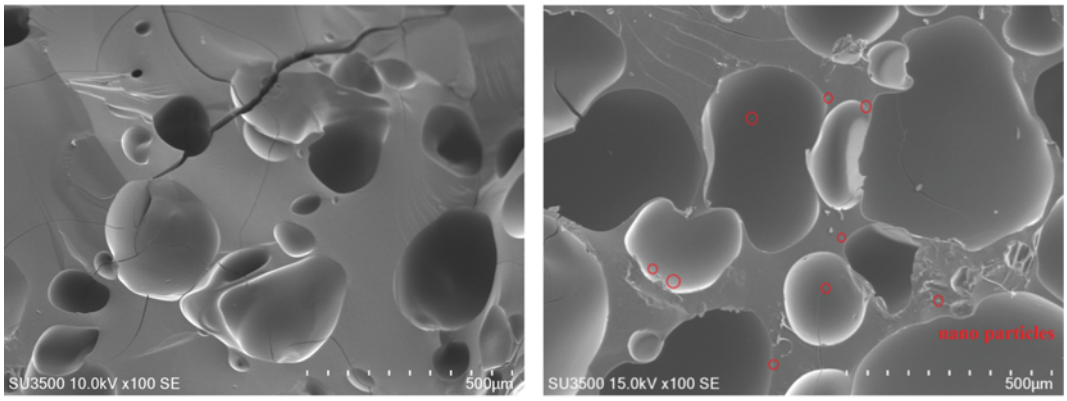

Fig. 3. The cross sectional SEM images of hydrogel with 100X magnification, (a): AMAH, (b): AMAH-co-SAC nanoparticles.

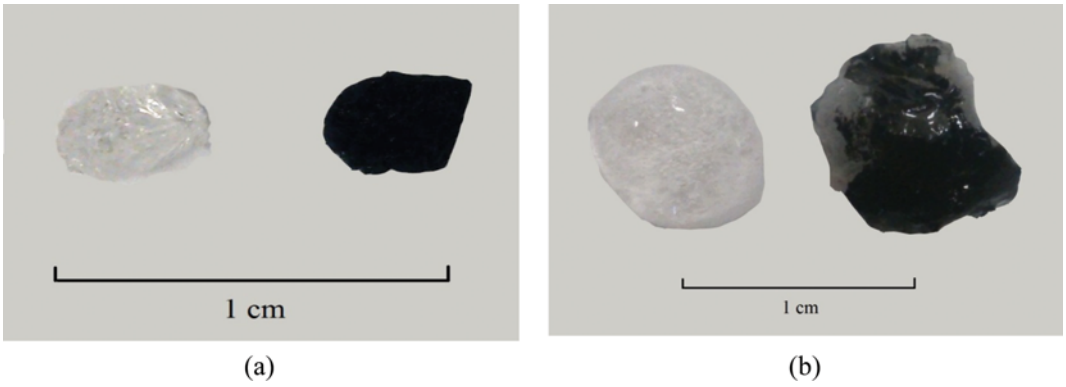

Fig. 4. Photograph of (a) dry AMAH (white) and AMAH-co-SAC (black), (b) swollen AMAH and AMAH-co-SAC nanoparticles in distillated water.

The characteristic bands at 1,640 cm^{-1} and 1,040 cm^{-1} are attributed to C=O stretching of the amide and S=O stretching, respectively. These bands and the band at 621 cm^{-1} are assigned to AMAH hydrogel, which are not present in the pristine membrane.

2. Hydrogel Morphological Analysis

To observe the internal structure of the prepared hydrogel, composite hydrogel and also the effect of super activated carbon nanoparticles on the hydrogel morphology, SEM was used. The related cross section SEM is shown in Figs. 3(a) and (b). The composite hydrogel (Fig. 3(b)) has more porous structure with wider voids rather than the plain hydrogel. Actually, adding nanoparticles increased the pores and free spaces in hydrogel structure. As void sizes in hydrogel are in micro scales (~200-600 μm), they cannot be filled by nanoparticles.

3. Hydrogel Swelling Measurements

Swelling ratio measurement was used to investigate the effect of nanoparticles on hydrogel structure. As it is clear, the swelling behavior is related to crosslink density. Figs. 4(a), (b) show the AMAH and composite AMAH in dry and swollen form. The hydrogel swelling ratio (based on Eq. (1)) was calculated 12.15 and 21.70 for AMAH and composite AMAH, respectively. Fig. 4 shows that the composite AMAH is more swollen. It could be attributed to the capacity of super activated carbon nanoparticles embedded in hydrogel to increase the pores and free spaces within the networks structure of the prepared hydrogel, and therefore, more water molecules could be accommodated [51].

4. Contact Angle and Surface Roughness

Membrane surface hydrophilicity was evaluated by contact angle measurement between the membrane surface and air-water interface. The changes of contact angle by coating a hydrophilic hydrogel layer on membrane surface are shown in Fig. 5. Obtained results show that there is a significant enhancement in contact angles for

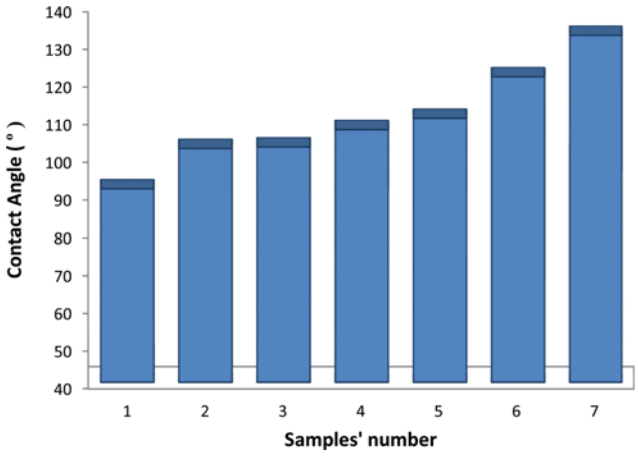

Fig. 5. Membrane surface hydrophilicity detected by water contact angle analysis.

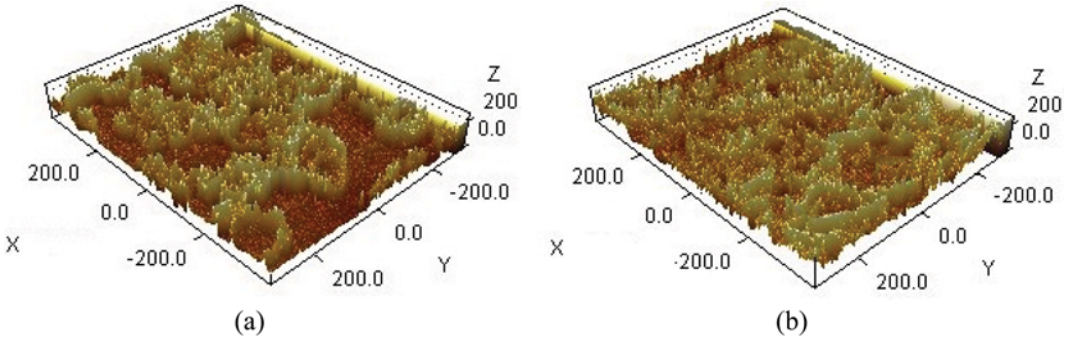

Fig. 6. Characterization of membrane surface roughness by 3D surface image metrology software, (a): Pristine membrane, (b): modified membrane coated with hydrogel layer containing SAC nanoparticles.

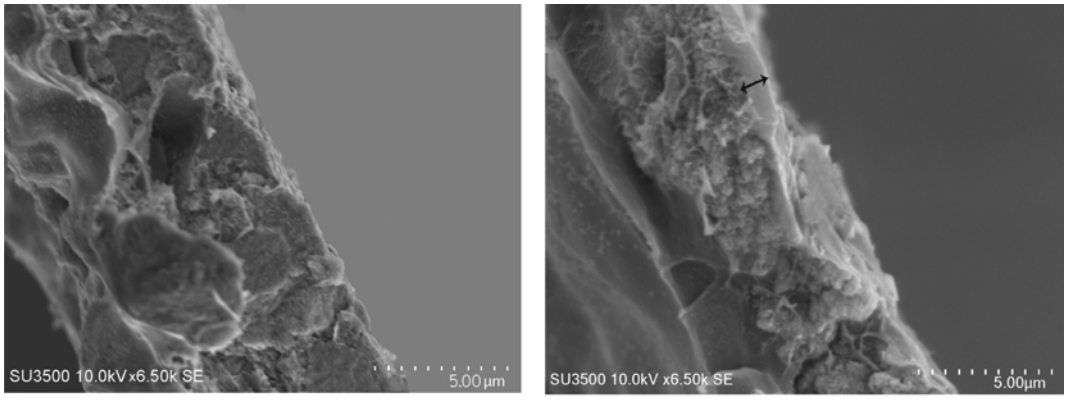

Fig. 7. The cross sectional SEM images of membranes: (a) pristine membrane, (b) modified membrane coated with hydrogel layer containing SAC nanoparticles.

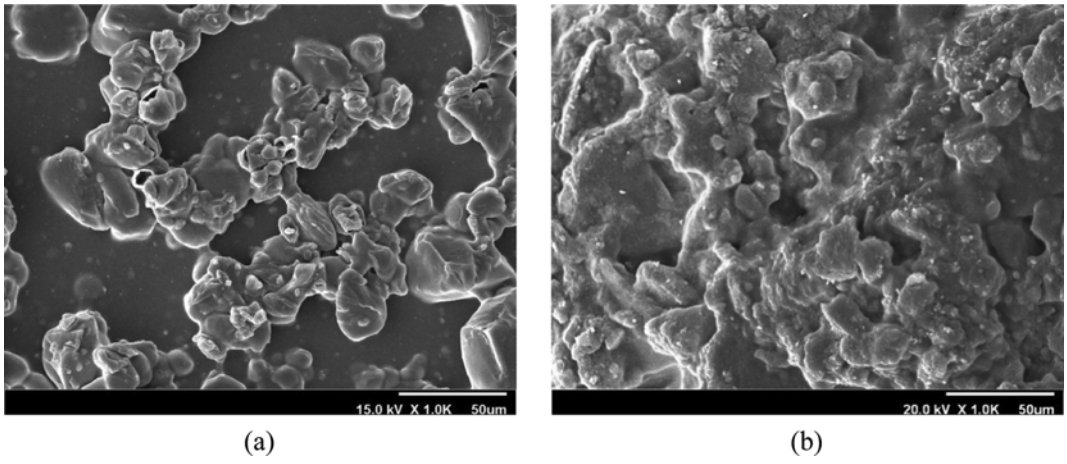

Fig. 8. The SEM surface images of (a) virgin membrane, (b) modified membrane coated with hydrogel layer.

the modified membranes. Therefore, the modified membrane surfaces are more hydrophilic. This is due to the relatively smoother membrane surface and the presence of a highly hydrophilic coated layer (hydrogel) on the surface of modified membranes. A more hydrophilic surface increases the solution interaction with the membrane, which can be responsible for the higher ionic transfer. The results show a decrease in the roughness of membrane surface and a more uniform surface after coating the thin layer on membrane surface (Fig. 6). Actually, by coating a hydrogel layer on membrane surface, free spaces between resins are filled by the hydrogel layer and a smoother surface is provided, which is in a good agreement with the hydrophilic characteristic of membrane surface.

5. SEM Analysis

SEM studies were performed to prove the formation of the modifier layer on membrane surface. The cross sectional SEM images are presented in Figs. 7(a), (b). The images reveal that a thin hydrogel layer was formed on the top surface of the membranes. Activated carbon nanoparticles residing on the membrane surface caused the formation of a thicker layer in some areas. The surface SEM images of unmodified membrane and modified with thin composite hydrogel layer with 1.0 K magnifications are presented in Figs. 8(a), (b). The polymer binder (PVC) and resin particles are clearly seen in Fig. 8(a). As Fig. 8(b) illustrates, the coated layer covers the membrane surface and fills the spaces between resins. This is responsible for the smoother membrane surface.

6. Water Content

The results for membrane water content (depicted in Fig. 9) revealed an increasing trend, i.e., the unmodified membrane showed 18.4% water uptake in the membrane structure while the modified one with a thin hydrogel layer shows 21.64%. The modifier coating layer contains a super hydrophilic hydrogel, which means high capacity of water adsorption on membrane surface. Membrane water content continued its increasing trend by adding super activated carbon nanoparticles in modifier solution. This might be attributed to the higher porous structure and the higher swelling ratio of the composite thin layer. As a consequence, membrane surface is more capable of adsorbing water molecules. The application of thin-film coatings usually decreases ionic permeability due to the presence of a thin, mass transfer resistant polymer layer [52], but the modifying layer used in this research can relatively reduce the mass transfer barrier effect since the higher amount of water content can provide more and wider pathway channels for

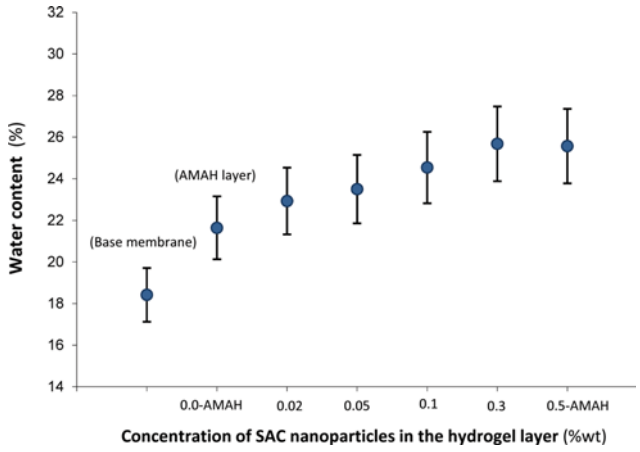

Fig. 9. The water content of prepared heterogeneous cation exchange membranes.

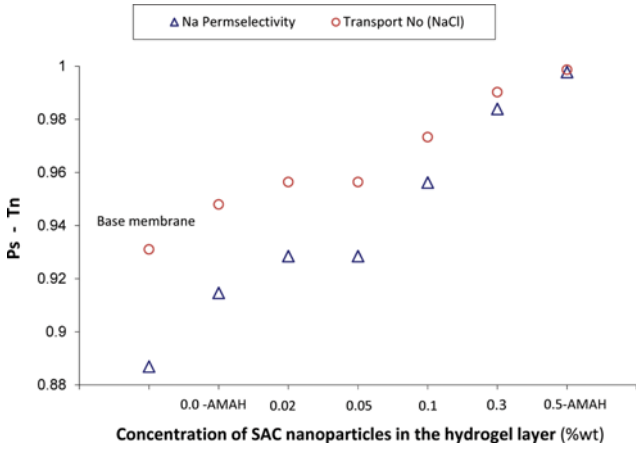

Fig. 11. Membranes' transport number and permselectivity in NaCl ionic solution.

ions transportation. Note that high water content in membrane structure leads to a loose structure for the membranes and relatively free pathways for co- and counter-ions transportation, which decreases the ionic selectivity, but this is not true for the prepared membranes in this research since the membrane structure does not adsorb more water, and the increased water content is due to the membrane surface. Water content measurements were made three times for each sample then their average value was reported.

7. Membrane Potential, Transport Number and Permselectivity

The obtained results (Figs. 10 and 11) indicate that potential, transport number and permselectivity of prepared membranes in NaCl solution had a remarkable improvement, which means that prepared membranes are highly selective. As seen in SEM images (Fig. 6(b)), the coating layer covers the membrane surface. Actually, the synergism between membrane functional groups and sulfonic groups of the modifier layer resulted in a stronger domination of ionic sites on membrane performance. Thus, dissociation of strongly acidic groups has a significant impact on the charged nature of membrane matrix and its domination on ionic transfer. Furthermore, embedding nanoparticles into modifier layer resulted in membrane potential, transport number and permselectivity improvement. The specific surface area of the prepared composite hydrogel increased markedly by loading nanoparticles, and sulfonic groups of the hydrogel are more accessible to the ions, and channels on membrane surface are stricter as the result. Therefore, co-ions are less likely to pass the membrane, so membrane potential, transport number and permselectivity increase.

8. Ionic Permeability and Flux

During the typical ED process, ions pass through the membrane and reach the concentrated section. Obtained results (Fig. 12) reveal an improvement in ionic permeability and flux of sodium ions by coating the hydrogel layer and adding nanoparticle to the surface modifier layer up to 0.05 wt% (sample 4). This desirable performance might be achieved in respect to the super hydrophilic nature of the coated hydrogel, which enhances the ionic interaction with membrane surface and provides more ionic transfer chances. Another factor might be the strong acidic functional groups of AMAH which provide a strong electrical field around membrane surface and increase ionic interaction and mobility in the solution noticeably. The super adsorbent characteristic of activated carbon nano-

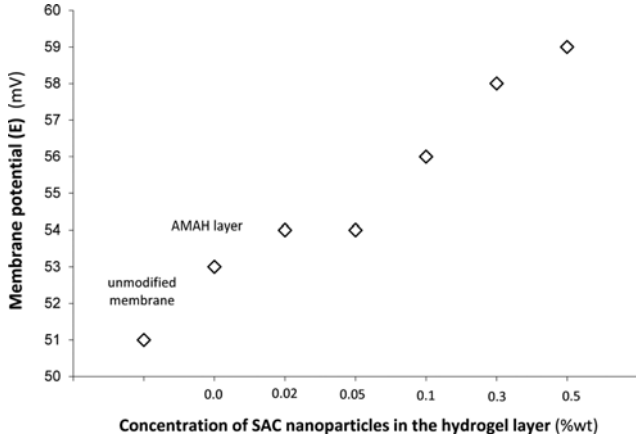

Fig. 10. The potential of prepared membranes in sodium chloride ionic solution.

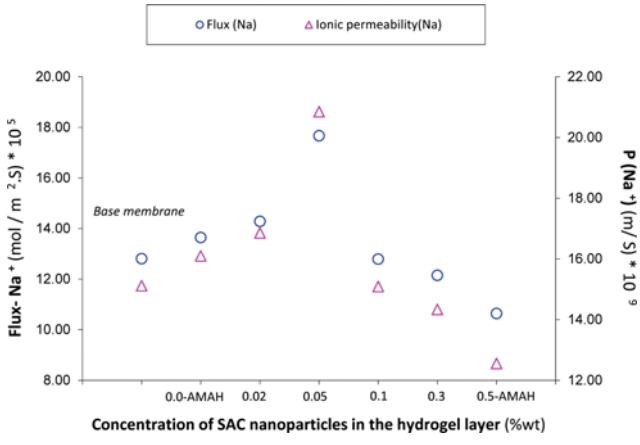

Fig. 12. Ionic permeability and flux for prepared membranes in NaCl ionic solution.

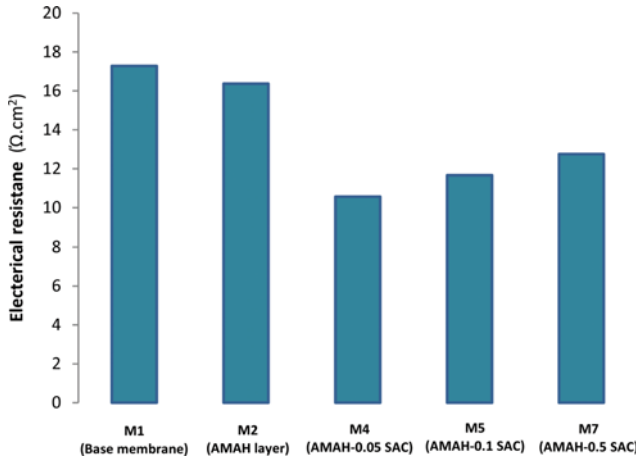

Fig. 13. Areal electrical resistance of pristine membrane (M_1) and the superior membranes (M_2, M_4, M_5, M_7) coated with hydrogel layer containing SAC nanoparticles.

particles, on the other hand, brings more ions to the membrane surface and makes more ionic interactions with membrane surface. Thus, the more ionic interactions with membrane surface results in a higher access of ions to the membrane surface, so ions spend longer time in contact with membrane surface and have higher chance to pass through it. Ionic permeability and flux of ions started to decline by increasing the concentration of nanoparticles in the modifying hydrogel layer. This might be attributed to the formation of void and free spaces in the hydrogel structure, which in turn enhances specific surface area of the modifier layer. Actually, the porous layer with activated sites has strength ionic site domination on ionic traffic and can reduce the permeability and flux.

9. Areal Electrical Resistance

The electrical resistance of pristine membrane (M_1) and superior membranes (M_2, M_4, M_5, M_7) were measured in 0.5 M NaCl solution at ambient temperature. The electrical resistance has practical implications due to its relation with energy consumption in the process. The modified membranes by the hydrogel layer and composite hydrogel layer on their surface showed lower electrical resistance compared to unmodified one (Fig. 13). Generally, selective membranes have higher electrical resistances, but in the present research this is not true [16]. The lower electrical resistance for the modified membranes can be explained with respect to the formation of a uniform electrical field around membrane surface due to the presence of functional groups of AMAH, which provides more conducting regions for the membrane. Moreover, the superior hydrophilic property of hydrogel layer and high adsorptive characteristic of super activated carbon nanoparticles increase the ionic interactions with membrane surface, which facilitates the ion traffic thorough the membrane and decreases the membrane electrical resistance.

CONCLUSION

Coating of a PVC based heterogeneous cation exchange membrane with a thin layer of hydrogel based on poly (2-acrylamido-2-methyl propane sulfonic acid) and super activated carbon nanoparticles caused the increase of membrane surface hydrophilicity, potential, permselectivity and transport numbers in sodium chloride ionic solution. Ionic flux and permeability were increased initially by increase of nanoparticles concentration up to the 0.05 wt. in the modifier solution and showed decreasing trend by more nanoparticle loading ratios. All membranes coated with a hydrogel containing SAC nanoparticles showed considerably lower electric resistance than the original uncoated membrane.

ACKNOWLEDGEMENT

The authors gratefully acknowledge Arak University for the financial support during this research.

REFERENCES

1. H. M. Hegab, Y. Wimalasiri, M. Ginic-Markovic and L. Zou, *Desalination*, **365**, 99 (2015).
2. L. A. Nezam, A. El-Din, A. El-Gendi, N. Ismail, K. A. Abed and A. I. Ahmed, *J. Ind. Eng. Chem.*, **26**, 259 (2015).
3. L. Zoua, I. Vidalis, D. Steele, A. Michelmore, S. P. Low and J. Q. J. C. Verberk, *J. Membr. Sci.*, **369**, 420 (2011).
4. J. Yin and B. Deng, *J. Membr. Sci.*, **479**, 256 (2015).
5. H. Farrokhzad, T. Kikhavani, F. Monnaie, S. N. Ashrafizadeh, G. Koeckelberghs, T. Van Gerven and B. Vander Bruggen, *J. Membr. Sci.*, **474**, 167 (2015).
6. X. Zuo, W. Shi, Z. Tian, S. Yu, S. Wang and J. He, *Desalination*, **311**, 150 (2013).
7. X. Zuo, S. Yu and W. Shi, *Desalination*, **290**, 83 (2012).
8. M. Reig, H. Farrokhzad, B. Vander Bruggen, O. Gibert and J. L. Cortina, *Desalination*, **375**, 1 (2015).
9. H. Farrokhzad, S. Darvishmanesh, G. Genduso, T. Van Gerven and B. Vander Bruggen, *Electrochim. Acta*, **158**, 64 (2015).
10. F. Q. Mir and A. Shukla, *Desalination*, **372**, 1 (2015).
11. A. H. Galama, N. A. Hoog and D. R. Yntema, *Desalination*, **380**, 1 (2016).
12. S. Mikhaylin, V. Nikonenko, N. Pismenskaya, G. Pourcelly, S. Choi, H. J. Kwon, J. Han and L. Bazinet, *Desalination*, **393**, 102 (2016).
13. S. M. Hosseini, A. R. Hamidi, A. R. Moghadassi, F. Parvizian and S. S. Madaeni, *Korean J. Chem. Eng.*, **32**(9), 1827 (2015).
14. S. Habibi, A. Nematollahzadeh and S. A. Mousavi, *Chem. Eng. J.*, **267**, 306 (2015).
15. S. M. Hosseini, M. Nemati, F. Jeddi, E. Salehi, A. R. Khodabakhshi and S. S. Madaeni, *Desalination*, **359**, 167 (2015).
16. S. M. Hosseini, A. R. Hamidi, S. S. Madaeni and A. R. Moghadassi, *Korean J. Chem. Eng.*, **32**(3), 429 (2015).
17. M. Nemati, S. M. Hosseini, E. Bagheripour and S. S. Madaeni, *Korean J. Chem. Eng.*, **33**(3), 1037 (2016).
18. S. Yu, Z. Lü, Z. Chen, X. Liu, M. Liu and C. Gao, *J. Membr. Sci.*, **371**, 293 (2011).
19. H. Z. Shafi, Z. Khan, R. Yang and K. Gleason, *Desalination*, **362**, 93 (2015).
20. H. Guo and M. Ulbricht, *J. Membr. Sci.*, **349**, 312 (2010).
21. S. M. Hosseini, S. S. Madaeni, A. R. Khodabakhshi and A. Zen-

dehnam, *J. Membr. Sci.*, **365**, 438 (2010).
22. P. Daraei, S. S. Madaeni, N. Ghaemi, H. Ahmadi Monfared and M. A. Khadivi, *Sep. Purif. Technol.*, **104**, 32 (2013).
23. Y. J. Choi, J. H. Song, M. S. Kang and B. K. Seo, *Electrochim. Acta.*, **180**, 71 (2015).
24. M. Moochani, A. R. Moghadassi, S. M. Hosseini, E. Bagheripour and F. Parvizian, *Korean J. Chem. Eng.*, **33**(9), 2674 (2016).
25. Y. J. Choi, M. S. Kang, S. H. Kim, J. Cho and S. H Moon, *J. Membr. Sci.*, **223**, 201 (2003).
26. N. Peng, Y. Wang, Q. Ye, L. Liang, Y. An, Q. Li and C. Chang, *Carbohydr. Polym.*, **137**, 59 (2016).
27. Z. Du, Y. Hu, X. Gu, M. Hu and C. Wang, *Colloid Surf., A. Physicochem. Eng. Asp.*, **489**, 1 (2016).
28. Y. Ma, T. Bai and F. Wang, *Mater. Sci. Eng.* C., **59**, 948 (2016).
29. S. M. Alshehri, A. Aldalbahi, A. B. Al-hajji, A. A. Chaudhary, M. Panhuis, N. Alhokbany and T. Ahamad, *Carbohydr. Polym.*, **138**, 229 (2016).
30. M. R. Guilherme, A. V. Reis, A. T. Paulino, A. R. Fajardo, E. C. Muniz and E. B. Tambourgi, *J. Appl. Polym. Sci.*, **105**, 2903 (2007).
31. C. Zhang, Z. Geng, M. Cai, J. Zhang, X. Liu, H. Xin and J. Ma, *Int. J. Hydrogen Energy*, **38**, 9243 (2013).
32. B. H. Kim, C. H. Kim and D. G. Lee, *J. Electro. Chem.*, **760**, 64 (2016).
33. L. Zhou, Y. Zhou and Y. Sun, *Int. J. Hydrogen Energy*, **29**, 475 (2004).
34. R. Mukherjee and S. De, *Sep. Purif. Technol.*, **157**, 229 (2016).
35. G. Skouteris, D. Saroj, P. Melidis, F. I. Hai and S. Ouki, *Bioresour. Technol.*, **185**, 399 (2015).
36. F. Bonvin, L. Jost, L. Randin, E. Bonvin and T. Kohn, *Water Res.*, **90**, 90 (2016).
37. A. Georgi, A. Schierz, K. Mackenzie and F. Dieter Kopinke, *J. Contam. Hydrol.*, **179**, 76 (2015).
38. H. M. Hegab, Y. Wimalasiri, M. Ginic-Markovic and L. Zou, *Desalination*, **365**, 99 (2015).
39. T. Sata, *Ion Exchange Membranes: Preparation, Characterization, Modification and Application*, The Royal Society of Chemistry, Cambridge Publications, United Kingdom (2004).
40. R. K. Nagarale, G. S. Gohil, V. K. Shahi and R. Rangarajan, *Colloid Surf., A. Physicochem. Eng. Asp.*, **251**, 133 (2004).
41. X. Li, Z. Wang, H. Lu, C. Zhao, H. Na and C. Zhao, *J. Membr. Sci.*, **254**, 147 (2005).
42. Y. Tanaka, *Ion Exchange Membranes: Fundamentals and Applications*, Elsevier, Netherlands, 12 (2007).
43. R. K. Nagarale, V. K. Shahi, S. K. Thampy and R. Rangarajan, *React. Funct. Polym.*, **61**, 131 (2004).
44. G. S. Gohil, V. V. Binsu and V. K. Shahi, *J. Membr. Sci.*, **280**, 210 (2006).
45. J. Kerres, W. Cui, R. Disson and W. Neubrand, *J. Membr. Sci.*, **139**, 211 (1998).
46. V. K. Shahi, S. K. Thampy and R. Rangarajan, *J. Membr. Sci.*, **158**, 77 (1999).
47. R. K. Nagarale, V. K. Shahi and R. Rangarajan, *J. Membr. Sci.*, **248**, 37 (2005).
48. S. M. Hosseini, A. Gholami, P. Koranian, M. Nemati, S. S. Madaeni and A. R. Moghadassi, *J. Taiwan Inst. Chem. Eng.*, **45**, 1241 (2014).
49. S. M. Hosseini, S. S. Madaeni, A. R. Heidari and A. R. Khodabakhshi, *Desalination*, **285**, 253 (2012).
50. N. Limparyoon, N. Seetapan and S. Kiatkamjornwong, *Polym. Degrad. Stab.*, **96**, 1054 (2011).
51. A. Hebeish, M. Hashem, M. M. Abd El-Hady and S. Sharaf, *Carbohydr. Polym.*, **92**, 407 (2013).
52. B. D. Mc Closkey, H. Bum Park, H. Ju, B. W. Rowe, D. J. Mille and B. D. Freeman, *J. Membr. Sci.*, **413**, 82 (2012).